Supporting Information:

A novel ruthenium(II) complex for two-photon absorption-based optical power limiting in the near-IR range.

Mickaël Four, Didier Riehl, Olivier Mongin, Mireille Blanchard-Desce, Latévi Max Lawson-Daku, Juliette Moreau, Jérôme Chauvin, Jacques A. Delaire, Gilles Lemercier

Table of Contents

.

S1 - Ligands PF, PFF, PTFF and PTFTF

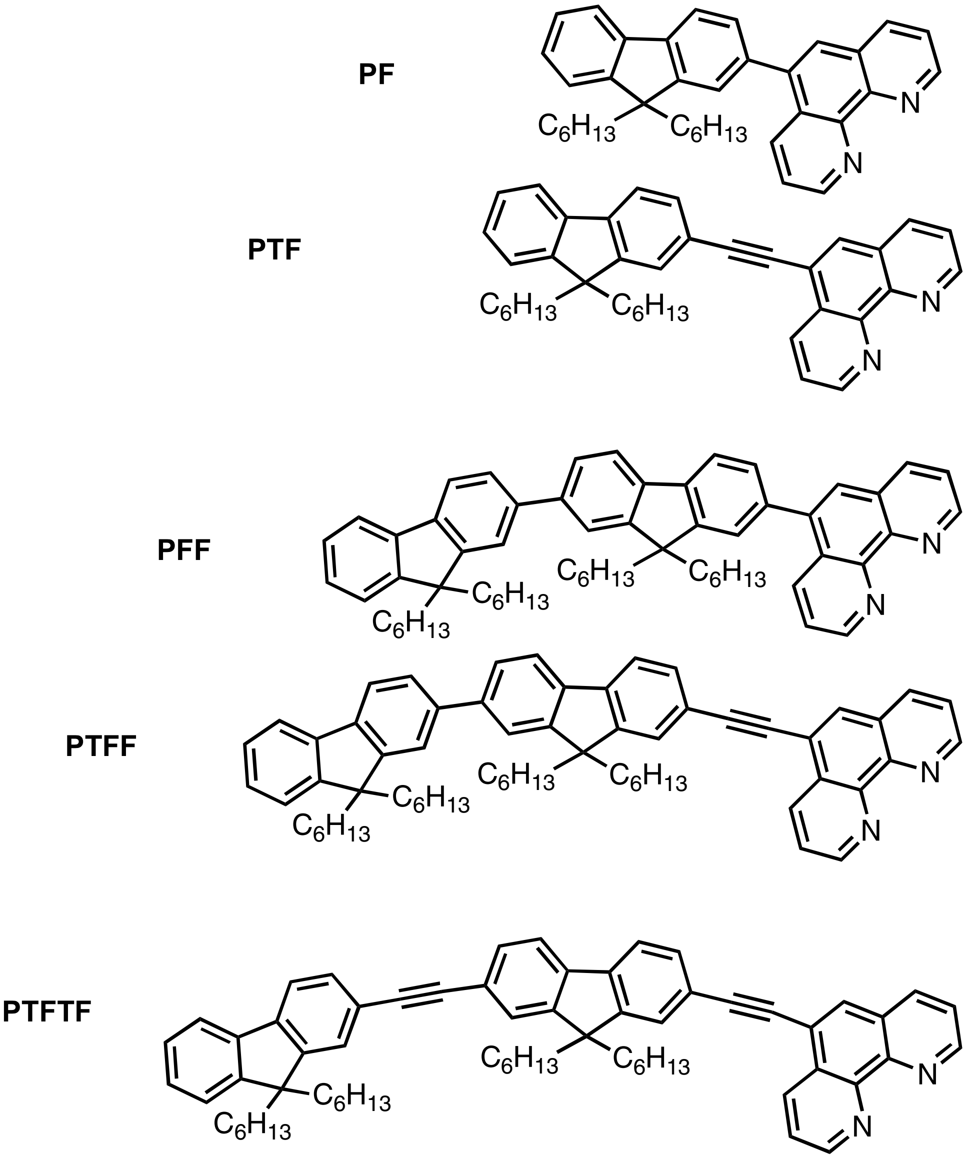

Figure S1 : Molecular structure of the **PF**, **PTF**, **PFF**, **PTFF**, and **PTFTF** ligands

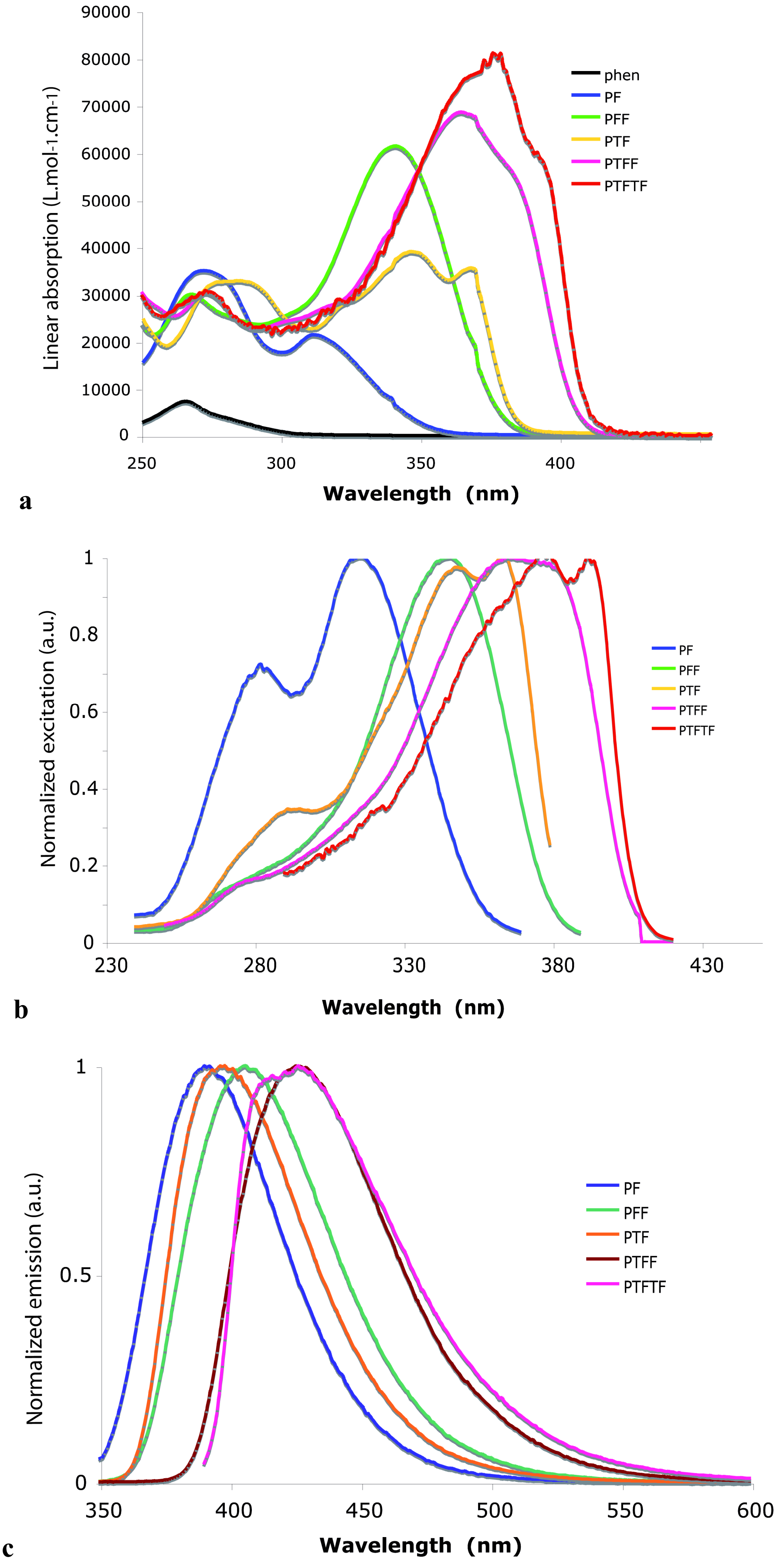

Figure S2. (a) Absorption spectra in $CHCl_3$; (b) Normalized excitation spectra in CH_2Cl_2, and (c) Normalized emission spectra in CH_2Cl_2 of the **PF**, **PTF**, **PFF**, **PTFF**, and **PTFTF** ligands.

S2 - Theoretical characterisation of the ligands PFF, PTFF and PTFTF

The ligands **PFF**, **PTFF** and **PTFTF** have been characterised theoretically using the models, which are shown in Figure S1, and which have been obtained by replacing the n-hexyl chains of the originals by hydrogen atoms. Density functional theory (DFT)[1] has thus been applied to the determination of the Onsager cavity radii of these models, and their lowest-lying excited singlet states have been characterised by electronic excitation calculations performed within time-dependent density-functional response theory (TDDFRT).[2]

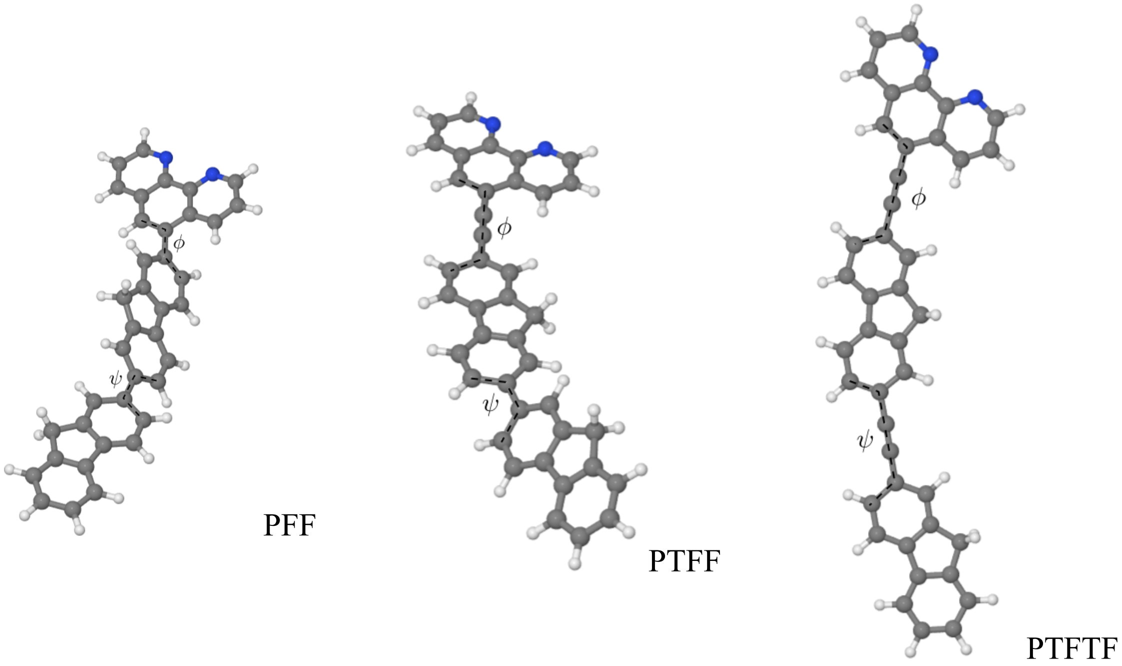

PFF

PTFF

PTFTF

Figure S3 Models used for the ligands **PFF**, **PTFF** and **PTFTF** and definitions of the angle φ, which gives a measure of the angle between the average planes of the **P** and the closest **F** moiety, and of the angle ψ, which gives a measure of the angle between the average plane of the **F** moieties.

---

[1] (a) P. Hohenberg and W. Kohn,. *Phys. Rev.* 1964, **136**, B864-B871. (b) W. Kohn and L. J. Sham, *Phys. Rev.* 1965, **140**, A1133-A1138.

[2] M. E. Casida in *Recent Advances in Density Functional Methods*, ed. D. P. Chong, Vol. 1, World Scientific, Singapore, 1995; pp 155-192.

S2.1 Computational details

The DFT and TDDFRT calculations were performed with the NWChem program package[3] using the PBE0 hybrid functional[4] and, for the description of all atoms, the Gaussian-type orbital (GTO) DFT basis set "DZVP2"[5] of double-ζ polarised quality. The geometries of the models have been optimised in their S_0 ground state with no symmetry constraint, except for the **PTFTF** model whose symmetry was constrained to C_s. Vibrational analyses performed on the calculated geometries led to real frequencies, indicating that these geometries correspond to true minima. The charge densities of the models have been calculated at the optimized geometries and used to estimate their Onsager cavity radii according to the formula $a= \square 3V_M/4\pi \square^{1/3} \square 0.5$, (in Å), where V_M is the molecular volume defined as the volume enclosed by the 0.001 au isodensity surface.[6] The TDDFT calculations were carried out with the Tamm-Dancoff approximation.[7] Molecular visualization and the calculation of the molecular volumes were done with the Jmol program.[8]

S2.2 Results

SI.2.1 Optimised geometries and estimates of the Onsager radii

For each ligand, there actually exist several rotamers, which differ by the values of the angles φ and ψ ((φ,ψ) in $[0,\pi]^2$). Thus, if one rotamer is characterised by the couple of angles (φ_0,ψ_0), the other rotamers will be characterised by angles values close to (φ_0,π-ψ_0), (π-φ_0,ψ_0), and (π-φ_0,π-ψ_0). For the

---

[3] (a) M. Valiev, E. Bylaska, N. Govind, K. Kowalski, T. P. Straatsma, H. J. J. Van Dam, D. Wang, J. Nieplocha, E. Apra, T. L. Windus and W. A. de Jong, *Comput. Phys. Commun.* 2010, **181**, 1477-1489. (b) W. A. de Jong, E. Bylaska, N. Govind, C. L. Janssen, K. Kowalski, T. Müller, I. M. B. Nielsen, H. J. J. van Dam, V. Veryazov and R. Lindh, *Phys. Chem. Chem. Phys.* 2010, **12**, 6896-6920.

[4] (a) J. P. Perdew, M. Ernzerhof and K. J. Burke,. *J. Chem. Phys.* 1996, **105**, 9982-9985. (b) C. Adamo and V. Barone, *J. Chem. Phys.* 1999, **110**, 6158-6170.

[5] N. Godbout, D. R. Salahub, J. Andzelm and E. Wimmer, *Can. J. Chem.* 1992, **70**, 560-571.

[6] M. W. Wong, K. B. Wiberg and M. J. Frisch, *J. Comp. Chem.* 1995, **16**, 385-394.

[7] S. Hirata and M. Head-Gordon, *Chem. Phys. Lett.* 1999, **314**, 291-299.

[8] B. McMahon and R. M. Hanson, *J. Appl. Cryst.* 2008, **41**, 811-814.

present study, the calculations have been limited for each ligand to the characterisation of only one of its rotamers because the rotamers are expected to have very similar physico-chemical properties. Table 1000 summarises the (φ,ψ) values found in the optimised geometries of the models as well as their calculated Onsager cavity radii.

The skeleton of the **PFF** model is not planar because of the steric interactions between neighbour H atoms pertaining to the **P** and the nearest **F** fragment ($\varphi > 0$) and because of similar interactions involving H atoms pertaining to the two **F** fragments ($\psi > 0$). On going to the **PTFF** model, the steric repulsion between the **P** and the nearest **F** fragment vanish, thanks to the insertion of the acetynyl (**T**) fragment. This translates into the planarity of the skeleton of the **PTF** moiety ($\varphi \sim 0$) , which is favourable to the delocalisation of the electronic .π cloud over the whole **PTF** moiety. The insertion of **T** between the two **F** fragments is expected to similarly lead to a planar **FTF** skeleton. This is the reason as to why the calculations on the **PTFTF** model has been done with the symmetry constrained to C_s ($\varphi = \psi = 0$). One also notes in Table 1000 that the predicted Onsager cavity radii slightly increase within the series, by 0.1 Å on going from the **PFF** to the **PTFF** model and also by 0.1 Å on going from the **PTFF** to the **PTFTF** model.

Table S1 Theoretical characterisation of the models of the ligands in their S_0 ground state :(φ,ψ) values found in the optimised geometries of the models and values of the Onsager cavity radius

	PFF	**PTFF**	**PTFTF**
(φ,ψ) (in deg)	(123.1, 36.5)	(0.1, 35.5)	(0.0,0.0)[a]
a (Å)	5.8	5.9	6.0

[a] The C_s symmetry used in the calculations imposes (φ, ψ) = (0.0,0.0).

S2.2.2 Lowest-lying $S_0 \rightarrow S_n$ electronic transitions ($n \leq 15$)

The features of the lowest-lying $S_0 \rightarrow S_n$ transitions of the **PFF, PTFF** and **PTFTF** models are summarised in Table S2, S3 and S4, respectively. These include the $S_0 \rightarrow S_n$ vertical excitation energies, the corresponding wavelengths, the associated oscillator strengths and the main characters of the transitions.

Table S2 Results of the TDDFRT calculations performed at the PBE0/DZVP2 level for the **PFF** model at its optimised C_1 geometry: excitation energies (E, in cm^{-1}), corresponding wavelengths (λ, in nm), oscillator strengths (f), and assignments based on the molecular orbital (MO) diagram shown Figure S2.

excited state	E	λ	f	major MO → MO transitions	main character
^{1}A	29461	339	1.59987	HOMO → LUMO (94%)	π[-FF] → π[PF-] CT
^{1}A	31310	319	0.00772	HOMO → LUMO+1 (75%) HOMO-1 → LUMO+1 (15%)	π[-FF] → π[P--] CT
^{1}A	32425	308	0.63478	HOMO → LUMO+2 (92%)	π[-FF] → π[PFF] CT
^{1}A	33240	301	0.00107	HOMO-3 →LUMO+1 (88%)	n[P--] → π[P--]
^{1}A	33381	300	0.00403	HOMO-3 → LUMO (65%) HOMO-3 → LUMO+2 (23%)	n[P--] → π[PF-]
^{1}A	34262	292	0.00601	HOMO-1 → LUMO+1 (31%) HOMO → LUMO+1 (17%) HOMO-4 → LUMO (14%) HOMO-2 → LUMO+1 (13%) HOMO-1 → LUMO (12%)	π[PFF] → π[P--] CT
^{1}A	34540	290	0.05687	HOMO-1 → LUMO (73%)	π[PFF] → π[PF-]
^{1}A	35185	284	0.02921	HOMO → LUMO+4 (56%) HOMO → LUMO+3 (20%)	π[-FF] → π[-F-] CT
^{1}A	35815	279	0.00358	HOMO → LUMO+3 (32%) HOMO → LUMO+5 (27%) HOMO → LUMO+4 (11%)	π[-FF] → π[-FF]
^{1}A	36772	272	0.00580	HOMO-1 → LUMO+2 (45%) HOMO-2 → LUMO (15%) HOMO-4 → LUMO+1 (11%)	π[PFF] → π[PFF]
^{1}A	36904	271	0.01316	HOMO-8 → LUMO (28%) HOMO-9 → LUMO (16%) HOMO-8 → LUMO+2 (11%)	nπ[PF-] → π[PF-]
^{1}A	37156	269	0.08024	HOMO-2 → LUMO (31%) HOMO-1 → LUMO+2 (24%) HOMO → LUMO+5 (11%)	π[PF-] → π[PF-]
^{1}A	37371	268	0.00356	HOMO-8 → LUMO+1 (50%) HOMO-9 → LUMO+1 (36%)	nπ[PF-] → π[P--] CT
^{1}A	37511	267	0.00265	HOMO-6 → LUMO (37%) HOMO → LUMO+7 (21%)	π[-F-] → π[PF-] CT
^{1}A	38306	261	0.00460	HOMO-5 → LUMO (35%) HOMO-5 → LUMO+2 (22%) HOMO → LUMO+8 (16%)	nπ[--F] → π[PF-] CT

Table S3 Results of the TDDFRT calculations performed at the PBE0/DZVP2 level for the **PTFF** model at its optimised C_1 geometry: excitation energies (E, in cm^{-1}), corresponding wavelengths (λ, in nm), oscillator strengths (f), and assignments based on the molecular orbital (MO) diagram shown Figure S3.

excited state	E	λ	f	major MO → MO transitions	main character
^{1}A	26280	381	2.35445	HOMO → LUMO (95%)	π[-TFF] → π[PTF-] CT
^{1}A	29810	335	0.01206	HOMO → LUMO+1 (76%) HOMO-1 → LUMO+1 (13%)	π[-TFF] → π[P---] CT
^{1}A	30772	320	0.51336	HOMO-1 → LUMO (55%) HOMO → LUMO+2 (39%)	π[PT-F] → π[PTF-] CT
^{1}A	31690	316	0.10381	HOMO → LUMO+2 (49%) HOMO-1 → LUMO (36%)	π[-TFF] → π[P-FF] CT
^{1}A	31916	313	0.00117	HOMO-3 → LUMO (82%) HOMO-3 → LUMO+2 (12%)	n[P---] → π[PTF-]
^{1}A	33376	300	0.00003	HOMO-3 → LUMO+1 (89%)	n[P---] → π[P---]
^{1}A	34013	294	0.00331	HOMO-1 → LUMO+1 (26%) HOMO-5 → LUMO (25%) HOMO → LUMO+1 (20%)	π[PT-F] → π[P---] + π[P---] → π[PTF-] CT
^{1}A	34237	292	0.01528	HOMO → LUMO+4 (69%) HOMO-9 → LUMO (12%)	π[-TFF] → π[--F-]
^{1}A	35043	285	0.04036	HOMO → LUMO+3 (36%) HOMO-2 → LUMO (23%)	π[-TFF] → π[---F] CT
^{1}A	35597	281	0.09264	HOMO-1 → LUMO+2 (54%) HOMO → LUMO+3 (17%) HOMO-6 → LUMO (10%)	π[PT-F] → π[P-FF] CT
^{1}A	35653	280	0.04496	HOMO → LUMO+5 (27%) HOMO-2 → LUMO (18%)	π[-TFF] → π[---F] CT
^{1}A	35658	280	0.00094	HOMO-8 → LUMO (70%)	n[P---] → π[PTF-]
^{1}A	36070	277	0.00977	HOMO-6 → LUMO (25%) HOMO-2 → LUMO (21%)	π[--F-] → π[PTF-] CT
^{1}A	36398	275	0.04129	HOMO-1 → LUMO+1 (23%) HOMO-5 → LUMO (23%) HOMO-6 → LUMO (12%)	π[PT-F] → π[P---] + π[P---] → π[PTF-] CT
^{1}A	36918	271	0.17731	HOMO → LUMO+3 (21%) HOMO-5 → LUMO (12%) HOMO → LUMO+5 (10%) HOMO-2 → LUMO (10%)	π[-TFF] → π[---F] CT **PTFTF**

Table S4 Results of the TDDFRT calculations performed at the PBE0/DZVP2 level for the **PTFTF** model at its optimised C_s geometry: excitation energies (E, in cm^{-1}), corresponding wavelengths (λ, in nm), oscillator strengths (f), and assignments based on the molecular orbital (MO) diagram shown Figure S4.

excited state	E	λ	f	major MO → MO transitions	main character
^{1}A'	24967	401	2.99603	HOMO → LUMO (95%)	π[-TFTF] → π[PTF--] CT
^{1}A'	29218	342	0.53509	HOMO → LUMO+1 (61%) HOMO-1 → LUMO (34%)	π[-TFTF] → π[P-FTF] CT
^{1}A'	29701	337	0.01090	HOMO → LUMO+2 (71%) HOMO-1 → LUMO+2 (17%)	π[-TFTF] → π[P----] CT
^{1}A'	30616	327	0.05358	HOMO-1 → LUMO (56%) HOMO → LUMO+1 (30%)	π[PT-TF] → π[PTF--] CT
^{1}A"	31750	315	0.00110	HOMO-3 → LUMO (73%) HOMO-3 → LUMO+1 (20%)	n[P----] → π[PTF--]
^{1}A'	33214	301	0.01298	HOMO-1 → LUMO+2 (22%) HOMO → LUMO+2 (18%) HOMO-4 → LUMO (15%) HOMO → LUMO+3 (14%)	π[PT-TF] → π[P----] CT
^{1}A"	33339	300	0.00002	HOMO-3 → LUMO+2 (89%)	n[P----] → π[P----]
^{1}A'	33426	299	0.00984	HOMO → LUMO+3 (33%) HOMO → LUMO+4 (30%)	π[-TFTF] → π[P-F-F] CT
^{1}A'	33810	296	0.17564	HOMO-1 → LUMO+1 (65%) HOMO-2 → LUMO (12%)	π[PT-TF] → π[P-FTF] CT
^{1}A'	34085	293	0.03998	HOMO → LUMO+4 (38%) HOMO → LUMO+3 (21%) HOMO-2 → LUMO (12%) HOMO-1 → LUMO+1 (10%)	π[-TFTF] → π[--F--] CT
^{1}A'	34958	286	0.00099	HOMO → LUMO+5 (47%) HOMO-2 → LUMO (13%)	π[-TFTF] → π[---F] CT
^{1}A'	35520	282	0.00765	HOMO-6 → LUMO (38%) HOMO → LUMO+7 (11%) HOMO-2 → LUMO (10%)	π[--F--] → π[PTF--] CT
^{1}A"	35558	281	0.00028	HOMO-8 → LUMO (63%) HOMO-8 → LUMO+1 (17%)	n[P----] → π[PTF--]
^{1}A'	35712	280	0.02549	HOMO-6 → LUMO (20%) HOMO-4 → LUMO (19%) HOMO-1 → LUMO+2 (14%) HOMO-2 → LUMO (11%)	π[--F--] → π[PTF--] + π[P----] → π[PTF--] CT
^{1}A'	36132	277	0.16715	HOMO-4 → LUMO (21%) HOMO-2 → LUMO (17%) HOMO-1 → LUMO+2 (16%) HOMO → LUMO+3 (13%)	π[--F--] → π[PTF--] CT

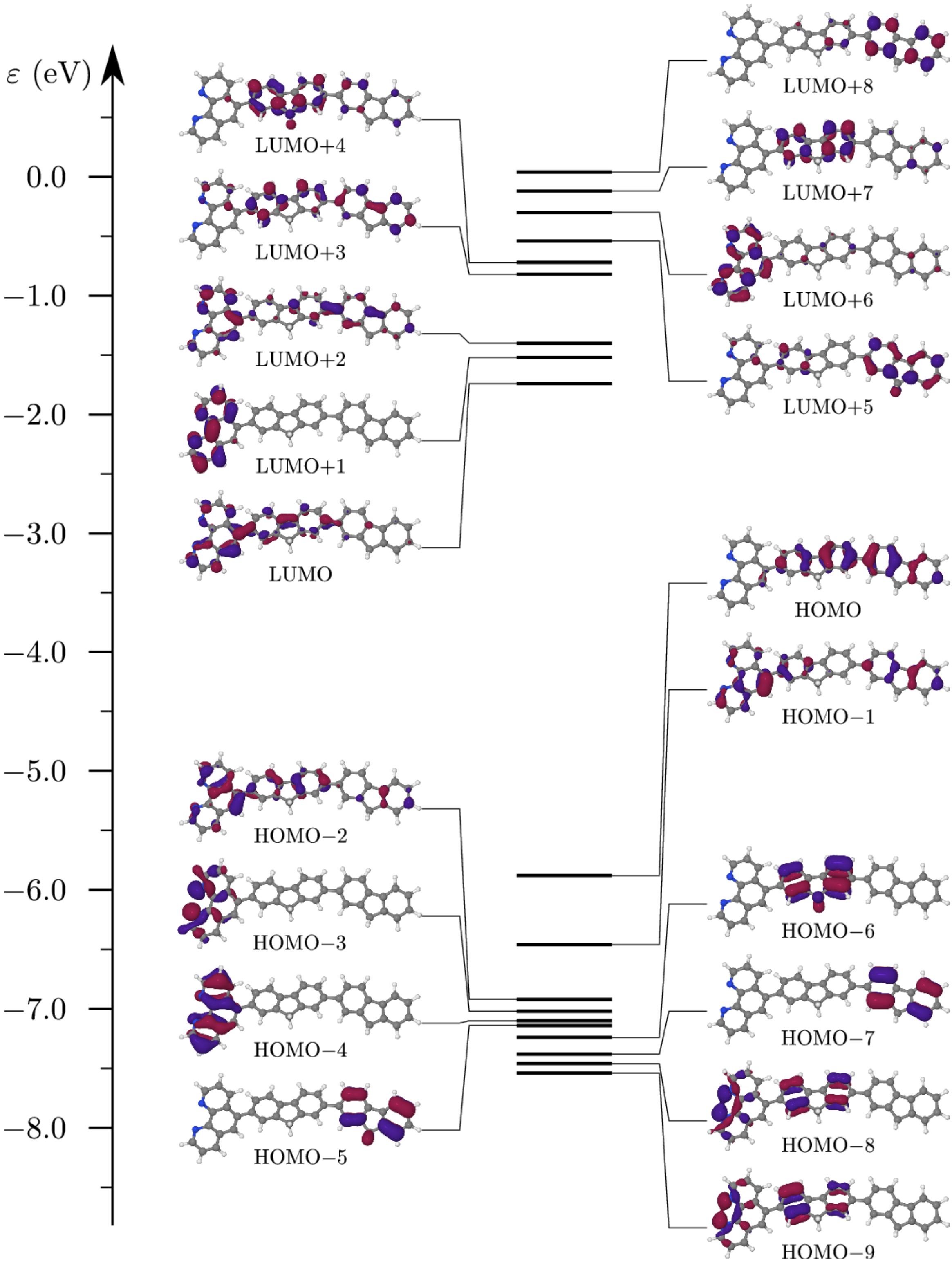

Figure S4 Diagram of the frontier Kohn-Sham molecular orbitals determined at the PBE0/DZVP2 level for the **PFF** model at its optimised *C*$_1$ geometry.

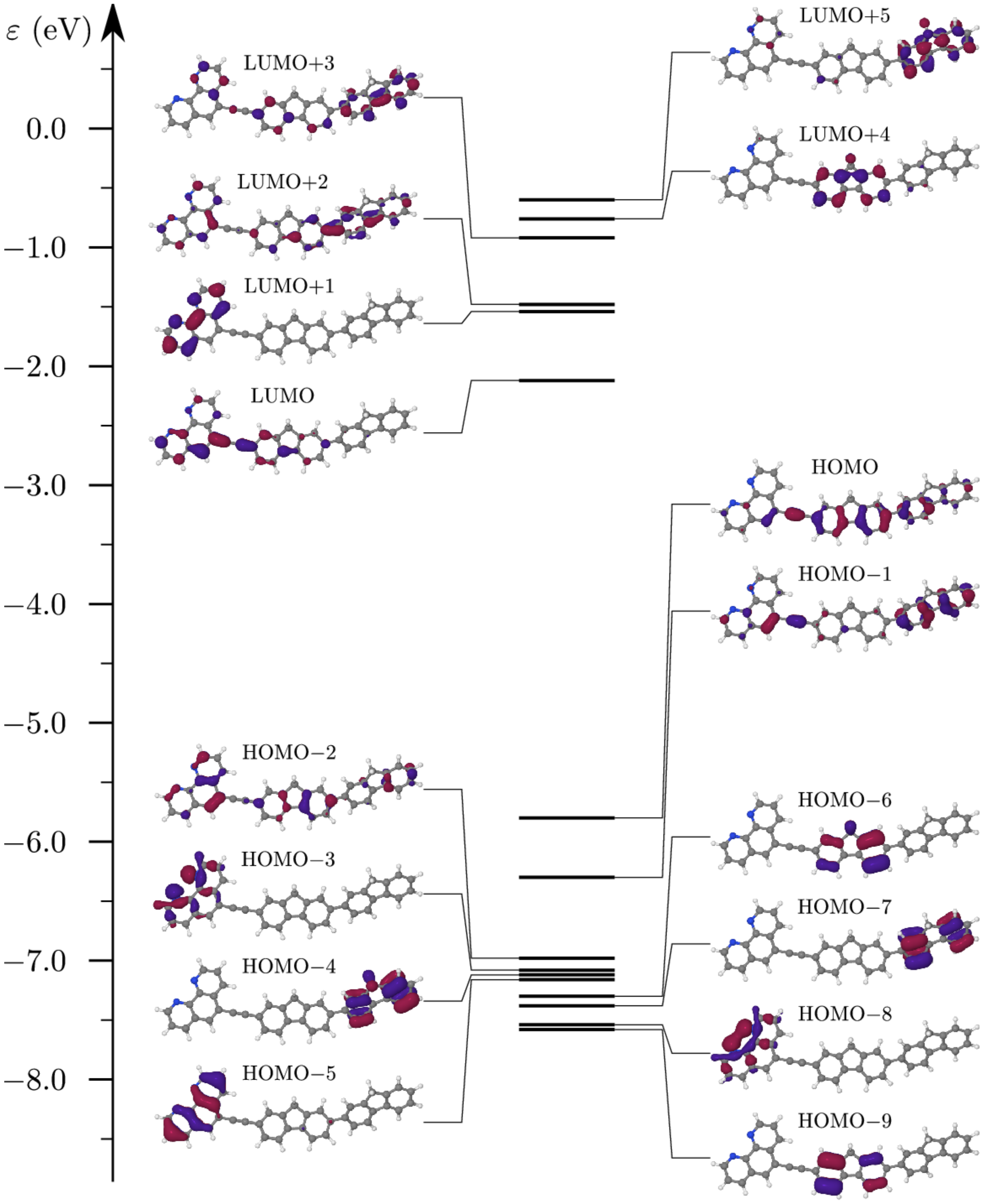

Figure S5 Diagram of the frontier Kohn-Sham molecular orbitals determined at the PBE0/DZVP2 level for the **PTFF** model at its optimised C_1 geometry.

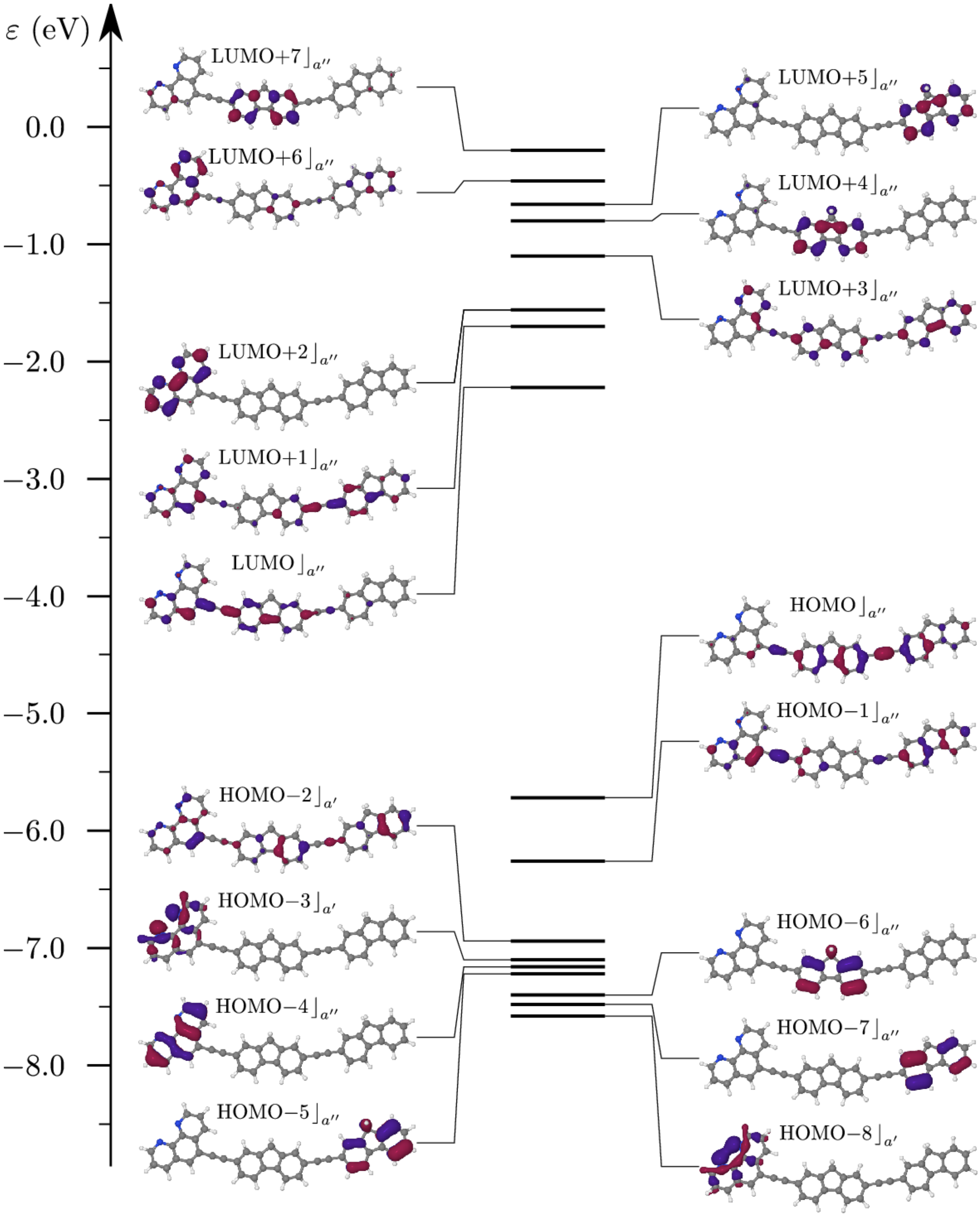

Figure S6 Diagram of the frontier Kohn-Sham molecular orbitals determined at the PBE0/DZVP2 level for the **PTFTF** model at its optimised C_s geometry (the symmetries of the orbitals, a' or a'', are indicated).